University of Tehran Press

Energy Estimation as Earthquake Precursor, Using the Energy of the Radiated Particles with the Help of Monte Carlo Methods

Bahari, A.[1] ✉ | Mohammadi, S.[1]

1. Department of Physics, Payame Noor University, Tehran, Iran.

Corresponding Author E-mail: aboozar.bahari@gmail.com

Abstract

In this study, utilizing the relationships between the energy of atomic/nuclear particles released from underground piezoelectric rocks and the elastic energy stored in these rocks, we introduced some methods to estimate the time/energy of incoming earthquakes in aseismic regions by measuring the energy of radiated particles. Since piezoelectric granite rocks make up approximately 60% of the Earth's crust, the increase in the energy of the detected particles in a certain period of time can be considered as an important precursor for the impending shallow earthquake. This analysis holds significant promise for enhancing the earthquake time and energy estimation methodologies. The detection of radiated particles from piezoelectric rocks can be achieved by utilizing detectors placed either on the surface or inside deep wells that are drilled near active faults. However, it is essential to note that the presented methodologies are approximations, as they rely on constant parameters for the piezoelectric material and presuppose that earthquakes occur within a piezoelectric block.

1. Introduction

Researchers have noted fluctuations in the Earth's electromagnetic fields and the radiation of various particles at different stages of earthquakes. This has led to the hypothesis that alterations in the energy and flux of these particles may act as indicators of impending seismic events. These anomalies could be detected using magnetometers, electric field sensors, nuclear particle detectors, and other monitoring devices. Researchers are investigating whether monitoring these signals could provide valuable insights into the build-up of stress along fault lines and the potential for an impending earthquake.

In some parts of the world, earthquakes are often accompanied by lightning. Finkelstein & Powell (1970) suggested that the piezoelectric effect in the Earth's crust causes the electrical field. In rock with a mean piezoelectric coefficient, several percent that of x cut single crystal quartz, and with typical seismic stress changes of 30–300 bars, an earthquake makes an average electrical field of 500–5,000 V cm^{-1}. For distances of half the

seismic wavelength, the generated voltage is 5×10^7 to 5×10^8 V, comparable with the voltage responsible for lightning in storms (Finkelstein & Powell (1970)).

The study of Mansouri Daneshvar & Freund (2019) affirms a process by which tectonic stresses deep in the Earth's crust lead to positive charges at the surface-to-air interface and air ionization, which can trigger atmospheric glows. Fu et al. (2015) identified abnormal changes in gamma-ray counting rates leading up to localized earthquakes in eastern Taiwan. Maksudov & Zufarov (2017) introduced a novel forecasting approach based on simultaneous monitoring of low-energy neutron and charged particle flux intensities through detectors. Volodichev et al. (2000) documented heightened neutron emissions in seismic zones of the Pamir region, exceeding typical levels by up to two orders of magnitude, particularly before significant earthquakes of magnitude 4 or greater on the Richter scale.

Sigaeva et al. (2006) observed neutron emissions preceding the December 2004

Sumatra earthquake. Borla et al. (2015) observed a strong correlation among acoustic, EM, and neutron emissions with major earthquakes in the vicinity of Testa Grigia Laboratory and the Val Trebbia seismic region in Italy. They noted a noteworthy increase in neutron dose rates, around six times greater than the natural background, and detected anomalous high-energy neutron components, particularly around 8 MeV, during seismic activity in granitic areas, thus reinforcing the piezo-nuclear hypothesis.

Bahari et al. (2022) employed piezoelectricity principles and elastic energy formulas along with the MCNPX simulation code to investigate the generation of atomic/nuclear particles, predominant interactions, and potential particle energies in quartz and granite blocks under mechanical stress. They demonstrated that in large granite blocks, nuclear particle creation is primarily driven by photonuclear interactions resulting from Bremsstrahlung gamma-ray photons due to runaway electron avalanches under stress conditions. Furthermore, they presented formulas to estimate the quantity and energies of various particles generated on a surface when a piezoelectric block is subjected to varying uniaxial stresses.

Bahari et al. (2024) also highlighted the estimation of particle flux from under-stressed granitic rocks using the MCNPX code at different distances from the earthquake hypocenter inside the fractures filled with air, water and CO_2. The study reveals that gases like air and CO_2 can facilitate particle flux far from the seismic source, with potential detection on the surface. Especially for deep earthquakes, the vacuum-filled fractures can facilitate the radiated nuclear particles to reach the surface.

In addition, Bahari & Mohammadi (2024) simulated the nuclear interactions between the created neutrons from under-stressed piezoelectric rocks and the elements of granite plus the elements of fractures' filling fluids. The results indicate that compound nuclear reactions like fusion/fission/inelastic scattering can happen, resulting in the release of energy from the depths of the Earth in the aseismic regions. Furthermore, compound nuclear interactions from the piezoelectric effect can generate some stable isotopes like deuterium (^2H), carbon (C) or oxygen (O) and also some radioisotopes in the granitic rock

texture or inside the fracture-filling fluids. Hence, their study illustrates that an increase in the amount of deuterium or CO_2 in the water/air of an aseismic region would be two important precursors of incoming earthquakes.

In this study, we aim to leverage the established relationships between accumulated elastic energy and the energy of radiated particles from piezoelectric rocks under mechanical stress to calculate the rate of elastic energy accumulation in rocks and faults. This analysis holds significant promise for enhancing earthquake time and energy estimation methodologies.

It is worth mentioning that the detection of radiated particles from piezoelectric rocks can be achieved by utilizing detectors placed either on the surface or inside deep wells that are drilled near active faults.

One might wonder how we can distinguish between piezo atomic/nuclear particles and geo-particles produced by natural radioactivity. The answer lies in the fact that in a region without seismic activity, there exists a relatively constant level of detected geo-particles (such as geo-neutrons), known as the background level. However, when mechanical stress is stored in the rock, the phenomenon of piezoelectricity leads to an increased flux of particles compared to the background level. Furthermore, the energy of the detected piezo-particles rises with an increase in mechanical force, whereas geo-particles generally possess lower average energy. This distinction allows us to discriminate between the two types of particles.

Another question arises regarding the amount of data acquisition time required with existing radiation detectors to obtain a signal that can be distinguished from background radiation signals. The answer lies in the fact that as energy accumulates in the underground piezoelectric rock, lower-energy atomic particles such as electrons or photons are emitted. As the energy accumulation increases, nuclear particles, along with higher-energy atomic particles, are also emitted. Therefore, the detection of neutrons and high-energy gamma rays serves as a precursor to strong earthquakes (Bahari et al., 2022). Furthermore, it is crucial to emphasize the significance of time in the early warning of an earthquake. Our previous study using

MCNPX simulation revealed that in a 2-kilometer deep air-filled vertical fracture when the source particles are neutrons with an energy of 24.6 MeV (Mega electron Volt) and travel from the bottom to the top surface of the fracture, the average time for the capture or escape of created photon particles is 1.87E-04 s. Additionally, their mean free path (*mfp*) is calculated to be 1.58E+04 cm (Bahari et al., 2024). Hence, once these particles are generated, they can be promptly accessed and identified, which could aid in providing early alerts for approaching earthquakes.

2. Materials and Methods
2-1. The mechanism of earthquake energy accumulation and its release
The process of earthquake energy accumulation and subsequent release involves the sudden transformation of stored elastic energy (E_{el}) from tectonic forces into kinetic energy (E_K) during rock sliding, along with residual potential energy after sliding stops (E_r) and energy dissipated (E_d) through friction and other processes (Kunquan et al., 2018). This relationship can be expressed as:

$$E_{el} = E_K + E_r + E_d \qquad (1)$$

The acoustic wave energy (E_{AC}) responsible for seismic damage originates from the kinetic energy of rock sliding. Assuming all potential energy is released, the residual energy (E_r) becomes zero. By substituting E_K with E_{AC}, we get:

$$E_{el} = E_K + E_d = E_{AC} + E_d \qquad (2)$$

The dissipated energy (E_d) comprises dissipated heat (Q), fracture energy (E_F), and particle radiation ($E_{radiation}$) released from rocks as a result of the piezoelectricity or other mechanisms. Therefore:

$$E_d = Q + E_F + E_{radiation} \rightarrow$$
$$E_{el} = E_{AC} + E_F + E_{radiation} + Q \qquad (3)$$

Gutenberg and Richter (1956) established a correlation between earthquake energy radiated in elastic waves in ergs (10^{-7} J) and the Richter scale magnitude (M_L) of the earthquake:

$$Log\ E_{AC} = 2.4\ m + 5.8$$
$$m = 1.7 + 0.8M_L - 0.01M_L{}^2 \qquad (4)$$

To determine the elastic energy stored in a rock block under mechanical load, we can simplify the calculation by assuming the block is experiencing uniaxial compressive stress ($\sigma_2 = \sigma_3 = 0$ and $\sigma_1 = \sigma$). The input elastic energy (E_{el}) per unit volume of rock in J/m^3 can be calculated using the following equation (Liang et al., 2015; Gao et al., 2020]:

$$E_{el}\ per\ unit\ volume = \frac{1}{2}\sigma\ \varepsilon_{el} = \frac{1}{2}\frac{\sigma^2}{\breve{E}} \qquad (5)$$

where ε_{el} represents the elastic strain and $\breve{E}$ is the elasticity modulus in GPa. The total input elastic energy in joules can then be determined by:

$$E_{el} = \frac{1}{2}\frac{\sigma^2}{\breve{E}}\ \mathbb{V} \qquad (6)$$

with $\mathbb{V}$ representing the rock volume in m^3.

Table 1 provides information on the elastic energy released and the corresponding Richter scale of an earthquake for three different cubic block sizes of granite, subjected to uniaxial stress at a rupture point of approximately 140 MPa and an elastic modulus of 40 GPa, assuming $E_{el} = E_{Ac}$ (no residual or dissipated energy) (Bahari et al., 2022).

It is important to consider that approximately 60% of the Earth's crust is composed of Granitic rocks.

Table 1. Elastic energy released and the corresponding Richter scale of an earthquake for three different cubic block sizes of granite, subjected to uniaxial stress at a rupture point (Bahari et al., 2022).

Length (m)	$\mathbb{V}$ (m^3)	E_{el} at rupture point (erg)	M_L
40	6.4E+4	1.57E+17	4.011
400	6.4E+7	1.57E+20	5.791
4000	6.4E+10	1.57E+23	7.670

2-2. Correlations between the energies of the radiated particles and the mechanical load applied on a piezoelectric block

In our prior research, we identified some relationships for the energy of atomic/nuclear particles, generated from piezoelectric blocks under stress using MCNPX (Monte Carlo N particles-extended) simulation, which is a nuclear physics code to simulate the particle's radiations (their energies and paths) through a material medium with three-dimensional geometry and continuous-energy transport. Some of these particles may travel into empty fractures while maintaining their initial energy until they are detected by near-logging tools located in deep wells or surface detectors. The equations representing these relationships are as follows (Bahari et al., 2022):

$$The\ average\ energy\ of\ created\ electrons, MeV = 0.0051\ ln(E_e) + 0.0019 \tag{7}$$

$$The\ average\ energy\ of\ created\ photons, MeV = 0.5193\ ln(E_e) - 1.6838 \tag{8}$$

$$The\ average\ energy\ of\ created\ neutrons, MeV = 4.4984\ ln(E_e) - 17.574 \tag{9}$$

$$The\ average\ energy\ of\ created\ protons, MeV = 2.4733\ ln(E_e) - 4.1223 \tag{10}$$

in which the piezoelectric relations are (Moheimani and Fleming, 2006; Halliday and Resnick, 1974):

$$E_e = \frac{U_P}{n_e} \tag{11}$$

$$U_P = V\ q \tag{12}$$

$$n_e = \frac{q}{e} \tag{13}$$

$$q = d\ F \tag{14}$$

$$V = \frac{q}{C_P} = \frac{d\ F}{C_P} = \frac{d\ F\ x}{\epsilon_0 \epsilon_r\ A} \tag{15}$$

where,
E_e: the potential energy of each electron, eV,
U_P: electric potential energy, J or eV,
V: electric voltage, V,
q: electric charge, C,
C_P: the capacitance of the piezoelectric material, Farad,
n_e: number of electrons on the negative charge surface,
e: charge of an electron $=1.602\times10^{-19}$ C,
d: matrix of piezoelectric coefficients, m/V or C/N,

F: applied force on the surfaces, N,
x: thickness of the piezoelectric material, m,
ϵ_0: vacuum permittivity $= 8.85\times10^{-12}$ F/m $=$ C^2/N/m^2,
ϵ_r: relative permittivity (dielectric constant), ($\epsilon = \epsilon_0\ \epsilon_r$),

According to Equations (7) to (10), once the energy of the particles being detected is determined, it becomes feasible to calculate the initial energy of the electrons (E_e) in the piezoelectric rocks under stress, along with their voltage. Subsequently, an estimation of the mechanical energy stored within the rock and the potential magnitude of an earthquake could be derived.

It must be taken into account that various particle detectors may apply different methods for particle detection. For instance, many photodetectors can be configured to detect individual photons, each with relative advantages and disadvantages. Common types include photomultipliers, Geiger counters, single-photon avalanche diodes, superconducting nanowire single-photon detectors, transition edge sensors, and scintillation counters (Hadfield, 2009; NIST, 2013).

3. Results and discussions

To forecast the occurrence of earthquakes, one can utilize Equations (7) to (10). To illustrate this, let us provide an example. Let's assume that the surface or downhole particle detectors in a seismically stable area record the average energy of the detected photons. Table 2 presents the assumed average energy of these photons based on the recording time. Furthermore, it is reasonable to assume that the energy of the emitted photons increases over time due to the gradual accumulation of elastic energy within the block or fault.

Table 2. Assumed average energy of detected photons, based on the recording time.

Recording time (days)	Detected photons' average energy (MeV)
1	0.0001
10	0.001
100	0.01
200	0.1
350	0.2
500	0.4
700	0.5

Based on the quantities provided in Table 2, the initial energy of the electrons (E_e) and the resulting voltage (V) can be calculated using Equation (10) and Equations (11) to (15), respectively. By applying Equation (15), the amount of applied force (F) can be estimated, assuming a constant size (x) for the piezoelectric cube. Subsequently, the uniaxial compressive stress ($\sigma_z = F_z/x^2$) on the block can be computed. Finally, Equation (6) can be used to evaluate the accumulated elastic energy (E_{el}) and the equivalent Richter magnitude (M_L) of the earthquake.

In Table 3, the computed piezoelectric and elastic energy parameters, along with the Richter magnitude (M_L), are presented for the incoming earthquake. These calculations are based on the assumed average energy of the detected photons, as provided in Table 2. The granite block used in the analysis has each side measuring 40 m. The piezoelectric coefficient is 7×10^{-13} C/N (Matsuda et al., 2005), the dielectric constant (ϵ_r) is 5 (Hubbard et al., 1997), the uniaxial compressive strength is 140 MPa, and the elastic modulus is 40 GPa.

It is important to recognize that the piezoelectric coefficient of rocks diminishes with increasing depth, attributed to the elevated temperatures found in the deeper crust. Hence, the quartz minerals present in granite exhibit the piezoelectric effect at depths reaching up to 23 km (Bahari et al., 2022). For the sake of simplicity, we have assumed that the piezoelectric coefficient remains constant across varying depths. Furthermore, as the depth increases, the uniaxial compressive strength of rocks tends to rise. Nevertheless, to simplify the description of methods, we have chosen to disregard the influence of depth on the uniaxial compressive strength of granite rock. Based on the information presented in Table 3 and depicted in Figure 1, the graph showcases the relationship between the calculated uniaxial compressive stress applied on a granite block, measuring 40 m on each side, and the corresponding recording day of the particles' energy. The graph suggests that a logarithmic function provides a better fit for the data. Assuming the uniaxial compressive strength of the granite rock is 140 MPa, it can be inferred that approximately on the 870th day, this block would experience rupture due to the uniaxial compressive stress. Consequently, an earthquake with a magnitude of approximately 4 on the Richter scale is expected to occur.

Table 3. Computed piezoelectric and elastic energy parameters for a granite block with each side of 40 m, along with the Richter magnitude (M_L) of the incoming earthquake

| Time (days)	Detected photons' Energy (MeV)	E_e (MeV)	Voltage (V)	F (N)	σ (MPa)	E_{el} (joule)	M_L
1	0.0001	25.60	25601074	64734145014	40.45	2619068457	3.39
10	0.001	25.64	25645482	64846433182	40.52	2628162435	3.39
100	0.01	26.09	26093818	65980083460	41.23	2720857133	3.40
200	0.1	31.03	31031681	78465823145	49.04	3848053376	3.48
350	0.2	37.62	37621495	95128639253	59.45	5655911254	3.58
500	0.4	55.29	55296489	1.39821E+11	87.38	12218716382	3.77
700	0.5	67.03	67039120	1.69513E+11	105.94	17959203977	3.87
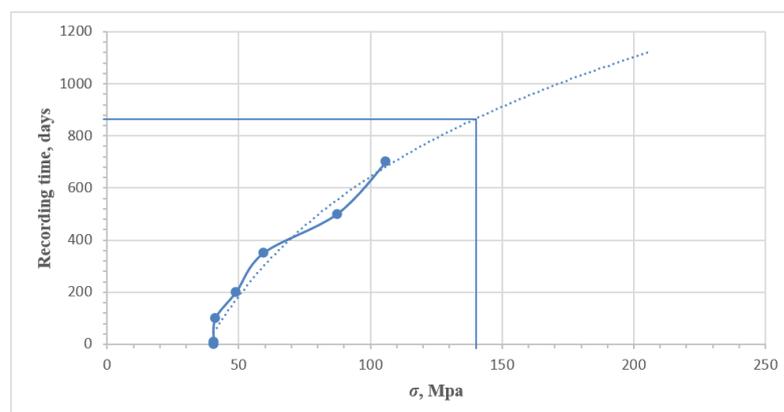
Figure1. Relationship between the calculated uniaxial compressive stress (σ) applied on a granite block with each side of 40 m and the recording time of the particles' energy. Logarithmic extrapolation was shown with a dashed line.

In the analysis mentioned above, a constant dimension was assumed for granite blocks (each side measuring 40 m) to determine the quantities of uniaxial mechanical stress. However, with the increase in elastic energy within the Earth's crust, the area affected by mechanical stress that could potentially rupture also increases (Mohajer-Ashjaei & Noroozi, 1978). If we were to consider a larger size for the granite block, such as 80 m for each side, the applied uniaxial stress (σ) would be half of the previous amount, resulting in double the elastic energy due to the applied stress and higher M_L quantities, as shown in Table 4. Consequently, the occurrence of an earthquake would be delayed to the 1320th day instead of the 870th day, as illustrated in Figure 2. Therefore, this method is only applicable when the size of the block affected by uniaxial compressive stress is known. The size of the block may be approximated using deep underground particle detectors or stress sensors spread across an area, enabling the creation of a 3D contour map illustrating the energies of detected particles or the amount of accumulated stress over time. The areas with high particle flux/energies experience greater stress, while areas with zero particle flux/energies are not affected by the underground stress. Through this approach, an approximate estimation of the block size can be derived. If this size is constant over time, it will be possible to apply the above-mentioned technique to predict the time of earthquake occurrence.

In addition, if there is already a fault in that block, one should first calculate the shear stress in the fault based on the amount of uniaxial compressive stress calculated according to the energy of the detected particles. Subsequently, by comparing this value with the shear strength of the fault-filling material, one can estimate the timing of a potential earthquake occurrence. Within the depth of 0-10 km, the average shear strength of fault gouge along the fault surface is approximately equal to or less than 10 MPa (Kunquan et al., 2018).

Table 4. Computed piezoelectric and elastic energy parameters for a granite block with each side of 80 m, along with the Richter magnitude (M_L) of the incoming earthquake

| Time (days)	Detected photons' Energy (MeV)	E_e (MeV)	Voltage (V)	F (N)	σ (MPa)	E_{el} (joule)	M_L
1	0.0001	25.60	25601074	1.29E+11	20.2	2619068457	3.56
10	0.001	25.60	25645482	1.29E+11	20.2	2628162435	3.56
100	0.01	26.09	2609381	1.31E+11	20.6	2720857133	3.57
200	0.1	31.00	31031681	1.56E+11	24.5	3848053376	3.65
350	0.2	37.60	37621495	1.90E+11	29.7	5655911254	3.75
500	0.4	55.29	55296489	2.79E+11	43.7	12218716382	3.94
700	0.5	67.03	67039120	3.3E+11	52.9	17959203977	4.04
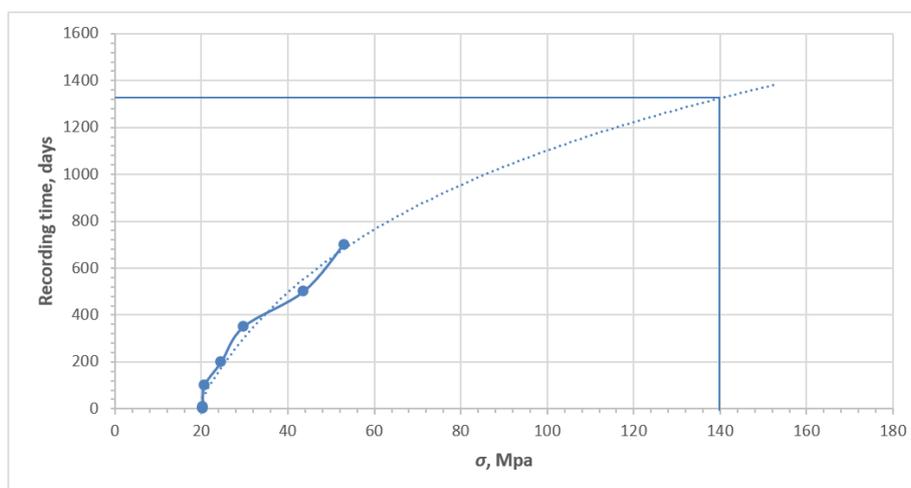
Figure 2. Relationship between the calculated uniaxial compressive stress (σ) applied on a granite block with each side of 80 m and the recording time of the particles' energy. Logarithmic extrapolation was shown with a dashed line.

Another method is considering if the piezoelectric rock with a variable size is fractured on a specific day, how much energy is released. Within this approach, we will not predict when the earthquake will happen, rather, we will estimate how much stored energy will be released if an earthquake happens on a particular day.

Upon obtaining data on the energy of detected particles, the energy of electrons (E_e) and the voltage produced (V) by the piezoelectric rocks can be calculated using Equation (10) and Equations (112) to (15), respectively. Subsequently, Equation (15) can be utilized to determine the value of F/x. By assuming that the final uniaxial compressive stress applied to the block would cause it to break and trigger an earthquake on that day (due to the elastic energy stress surpassing the final uniaxial strength of the block; i.e., $\sigma = F/x^2 = 140$ MPa), the size of the block (parameter x for each side) can be estimated. Through the computation of the force (F), the amount of elastic energy (E_{el}) released on that specific day can be evaluated.

The outcomes of this methodology for the provided data are presented in Table 5. As indicated in the table, for a granite block with a piezoelectric coefficient of 7×10^{-13} C/N, uniaxial compressive strength of 140 MPa, and elastic modulus of 40 GPa, over a 700-day period, the values of V, F, E_{el}, x, and M_L increase as the energy of detected photons rises. On the 700th day, the detected photons' energy suggests that if an earthquake were to occur on that day, a cubic granite block with a volume of 30.27^3 m^3 would rupture, releasing elastic energy amounting to 6.7×10^9 J and resulting in an earthquake with a magnitude of approximately 3.8 on the Richter scale.

It is important to acknowledge that the aforementioned analyses for earthquake prediction assume a constant uniaxial compressive strength and constant piezoelectric and dielectric coefficients for granitic rocks. However, it should be noted that these parameters may vary for different types of rocks. Additionally, the mechanism of stress that affects the Earth's crust, such as shear or tension stress, tri-axial stress, etc., may differ as well. Furthermore, as the depth increases, the piezoelectric coefficient decreases due to rising temperatures. Consequently, the results obtained from both analyses will inevitably be approximate.

It should be considered that there are many reports of earthquake precursors in the scientific literature, of about twenty different types that range from meteorology to zoology, and so far none of them have been completely reliable for earthquake prediction. However, our study introduces methods to estimate the time or energy of an impending earthquake, based on the detected particle energy. These methods can have appropriate reliability compared to other methods, because from our previous study, using elastic energy and piezoelectric formulas and applying Monte Carlo simulation, we know that there is a relationship between the increase in the energy of radiated atomic/nuclear particles and the elastic energy, stored in a granite block. Since granite rocks make up approximately 60% of the Earth's crust, the increase in the energy of the detected particles in a certain period of time can be considered as an important precursor for the impending shallow earthquake.

Table 5. Computed piezoelectric and elastic energy parameters for a granite block with variable size, along with the Richter magnitude (M_L) of the incoming earthquake.

Time (days)	The energy of crossing photons (MeV)	E_e (MeV)	Voltage (V)	F (N)	σ (MPa)	x (m)	E_{el} (joule)	M_L
1.00	0.0001	25.6	25601074	18707631833	140	11.56	378444547	3.09
10.00	0.001	25.6	25645482	18772588823	140	11.58	380417320	3.09
100.00	0.01	26.0	26093818	19434693809	140	11.78	400719599	3.10
200.00	0.1	31.0	31031681	27486095543	140	14.01	673974722	3.23
350.00	0.2	37.6	37621495	40399366098	140	16.99	1200980226	3.37
500.00	0.4	55.3	55296489	87276545588	140	24.97	3813470170	3.66
700.00	0.5	67.0	67039120	128280028403	140	30.27	6795362073	3.80

Besides, to enhance the accuracy of these methods, it would be advantageous to drill deep holes around faults and install long-term or permanent logging detectors downhole, close to the earthquake hypocenter, to monitor and detect the radiated particles with their initial energies. This proposal is completely operational and has already been implemented in projects such as SAFOD (San Andreas Fault Observatory at Depth) in the United States in a period of time and useful information was obtained from the behavior of the San Andreas Fault (Zoback et al., 2011).

4. Conclusion
This study has introduced methods to estimate the time/energy of earthquakes in aseismic regions by measuring the energy of radiated particles from underground piezoelectric rocks using particle detectors on the surface or downhole. As the energy of the detected particles rises, the stored elastic energy of the granite block also increases, potentially reaching a critical rupture point, at which point this energy is released suddenly, leading to the occurrence of an earthquake.

It should be mentioned that the most detected particles are likely to pass through vacuum-filled or lightweight fluid-filled fractures and reach the detectors.

Furthermore, it is important to note that the introduced methods are approximate estimations, as they assume constant parameters for the piezoelectric rock. In addition, we have supposed the earthquake happened in a piezoelectric block. If the earthquake does not occur in such types of rocks and does not emit any atomic or nuclear particles, it cannot be predicted using the mentioned approaches.

Continued research into particles' radiation anomalies and their potential role in earthquake prediction could contribute to our understanding of these complex natural phenomena in the future.

Data availability statement
The data that support the findings of this study are available from the corresponding author upon reasonable request

Funding and/or Conflicts of interests/ Competing interests

References
Bahari, A., Mohammadi, S., Shakib, N. S., Benam, M. R., & Sajjadi, Z. (2024). Monte Carlo Methods to Simulate the Propagation of the Created Atomic/ Nuclear Particles from Underground Piezoelectric Rocks through the Fractures Before the Earthquakes. *Atom Indonesia*, 50(1), 27-35, DOI: 10.55981/aij.2024.1311.

Bahari, A., & Mohammadi, S. (2024). Simulating the interactions between the produced neutrons from piezoelectric rocks and the surrounding medium during earthquakes', Iranian Journal of Physics Research, 24(3), pp. 53-60. doi: 10.47176/ijpr.24.3.11823

Bahari, A., Mohammadi, S., Benam, M. R., & Sajjadi, Z. (2022). Simulation with Monte Carlo Methods to Find Relationships between Accumulated Mechanical Energy and Atomic/Nuclear Radiation in Piezoelectric Rocks with Focus on Earthquakes. *Radiation effects and defects in solids*, 177(7-8), 743-767, DOI: 10.1080/10420150.2022.2073885.

Borla, O., Lacidogna, G., & Carpinteri, A. (2015). Chapter: Piezonuclear neutron emissions from earthquakes and volcanic eruptions, Book: *Acoustic, Electromagnetic, Neutron Emissions from Fracture and Earthquakes* (by Carpinteri A. et al.), Publisher: Springer International Publishing Switzerland.

Finkelstein, D. & Powell, J. (1970), Earthquake Lightning. Nature, 228, 759–760. https://doi.org/10.1038/228759a0

Fu, C. C., Wang, P. K., Lee, L. C., Lin, C. H., Chang, W. Y., Giuliani, G., & uzounov, D. (2015). Temporal variation of gamma rays as a possible precursor of earthquake in the Longitudinal Valley of eastern Taiwan. *Journal of Asian Earth Sciences*, 114(2), 362-372. DOI: 10.1016/j.jseaes.2015.04.035.

Gao, L., Gao, F., Xing, Y., & Zhang, Z. (2020). An Energy Preservation Index for Evaluating the Rockburst Potential Based on Energy Evolution, Energies, 13(14), 3636. DOI: 10.3390/en13143636.

Gutenberg, B., & Richter, C. F. (1956). Earthquake magnitude, intensity, energy,

and acceleration (Second paper). *Bulletin of the Seismological Society of America*, 46(2), 105-145.

Hadfield, R.H. (2009). Single-photon detectors for optical quantum information applications. *Nature Photonics*. 3(12), 696-705.

Halliday, D., & Resnick R. (1974). Fundamentals of Physics. Publisher: Wiley, New York.

Hubbard, S. S., Peterson, J. E., Majer, E. L., Zawislanski, P. T., Williams, K. H., Roberts, J., & Wobber, F. (1997). Estimation of permeable pathways and water content using tomographic radar data. *The Leading Edge*, 16(11), 1623-1628.

Kunquan, L., Zexian, C., Meiying, H., Zehui, J., Rong, S., Qiang, W., Gang, S. & Jixing, L. (2018). The mechanism of earthquake. *International Journal of Modern Physics B*, 32(7), pages (id): 1850080, DOI: 10.1142/S0217979218500807

Liang, C., Wu, S., Li, X., & Xin, P. (2015). Effects of strain rate on fracture characteristics and mesoscopic failure mechanisms of granite. *Int. J. Rock Mech. and Min. Sci.*, 76, 146-154.

Maksudov, A. U., & Zufarov, M. A. (2017). Measurement of neutron and charged particle fluxes toward earthquake prediction. *Earthquake Sci.*, 30(5-6), 283-288, DOI: 10.1007/s11589-017-0198-z.

Mansouri Daneshvar, M.R., & Freund, F.T. (2019). Examination of a relationship between atmospheric blocking and seismic events in the Middle East using a new seismo-climatic index. *Swiss J. Geosci.*, 112, 435-451.

Matsuda, T., Yamanaka, C., & Ikeya, M. (2005). Piezoelectric Measurements of Granite as Composite Material Using Atomic Force Microscope. *Japanese Journal of Applied Physics*, 44(2), 968-971.

Moheimani, R. S. O., & Fleming, A. J. (2006). Piezoelectric Transducers for Vibration Control and Damping, Chapter: Fundamentals of Piezoelectricity, Springer London, 9-35.

Mohajer-Ashjai, A., & Nowroozi, A. A. (1978). Observed and probable intensity zoning of Iran. *Tectonophysics*, 49(3–4), 149-160, DOI: 10.1016/0040-1951(78)90173-7.

National Institute of Standards and Technology (NIST) (2013), High Efficiency in the Fastest Single-Photon Detector System (Press release) Retrieved 2018-10-11.

Sigaeva, E., Nechaev, O., Panasyuk, M., Bruns, A., Vladimirsky, B., & Kuzmin, Y. (2006). Thermal neutrons' observations before the Sumatra earthquake. *Geophys. Res. Abstr.*, 8, 00435.

Volodichev, N. N., Kuzhevskij, B.M., Nechaev, O.Y., Panasyuk, M.I., Podorolsky, A.N., & Shavrin, P.I. (2000). Sun-Moon-Earth connections: the neutron intensity splashes and seismic activity. *Astron. Vestnik*, 34, 188-190.

Zoback, M. D., Hickman, S., Ellsworth, W., and the SAFOD Science Team (2011). Scientific drilling into the San Andreas Fault Zone—An overview of SAFOD's first five years. *Sci. Drill.*, 11, 14-28, DOI:10.2204/iodp.sd.11.02.2011.